Macromolecular Rapid Communication
www.mrc-journal.de

Naphthalimide-Based Aggregation-Induced Emissive Polymeric Hydrogels for Fluorescent Pattern Switch and Biomimetic Actuators

Hao Liu, Shuxin Wei, Huiyu Qiu, Beibei Zhan, Qingquan Liu, Wei Lu, Jiawei Zhang, To Ngai, and Tao Chen**

Substituted naphthalimide (NI) moieties are highly versatile and newly recognized aggregation-induced emission (AIE) building blocks for many potentially useful smart molecules, polymers, and nanoparticles. However, the introduction of NI fluorophore into cross-linked polymeric networks to prepare AIE-active hydrogels still remains underdeveloped. Herein, a novel naphthalimide-based aggregation-induced emissive polymeric hydrogel is reported, followed by its proof-of-concept applications as fluorescence pattern switch and biomimetic actuator. The hydrogel, bearing semi-interpenetrating polymer networks, is synthesized starting from *N*-isopropylacrylamide, hydroxyethyl methacrylate, and a newly designed NI monomer (4-phenoxy-*N*-allyl-1,8-naphthalimide, PhAN). Rational molecular design for AIE-active PhAN monomer lies in modification of the NI core with rigid and bulky phenoxy group to break its planarity to produce desirable propeller-shaped molecular conformation. The as-prepared hydrogel is proved to be a aggregation-induced blue-light-emitting hydrogel. It also shows volume phase transition behavior and is endowed with thermally responsive synergistic emission and transmittance change, thus enabling simultaneous regulation of two optical properties merely by one single stimulus. These useful advantages further encourage fabrication of several proto-type fluorescence pattern switching and biomimetic actuating devices. This study may not only enlarge the list of fluorescent hydrogels but also serve as a novel smart optical platform for potential anticounterfeiting, sensing, displaying, or actuating applications.

Many marine mollusks are found to exist in a gel state and have evolved to exhibit smart luminescent behavior for camouflage, communication or reproduction purposes.[1,2] For example, Atolla Jellyfish is reported to show striking bioluminescent patterns for help when captured by predators. Watasenia Scintillans are known to have amazingly synergistic control over shape and skin color to camouflage themselves in response to external stimuli. Such interesting fluorescence pattern switching and synergistic color/shape actuating behaviors of natural mollusks have inspired the development of artificial polymeric hydrogels with responsive fluorescence. Over the past decades, a number of fluorescent polymeric hydrogels have been designed and constructed by introducing luminescent nanoparticles,[3–6] lanthanide complexes,[7–13] and especially organic fluorogens[14–27] into the cross-linked hydrogel network. Among them, AIEgens-based polymeric hydrogels are of particular research interest because significantly enhanced emission can be

H. Liu, S. X. Wei, H. Y. Qiu, B. B. Zhan, Prof. W. Lu, Prof. J. W. Zhang, Prof. T. Chen
Key Laboratory of Marine Materials and Related Technologies
Zhejiang Key Laboratory of Marine Materials and Protective Technologies
Ningbo Institute of Materials Technology and Engineering
Chinese Academy of Sciences
Ningbo 315201, China
E-mail: luwei@nimte.ac.cn; tao.chen@nimte.ac.cn

H. Liu, S. X. Wei, Prof. W. Lu, Prof. J. W. Zhang, Prof. T. Chen
School of Chemical Sciences
University of Chinese Academy of Sciences
Beijing 100049, China

B. B. Zhan, Prof. Q. Q. Liu
School of Materials Science and Technology
Hunan Provincial Key Laboratory of Advanced Materials for New Energy Storage and Conversion
Hunan University of Science and Technology
Xiangtan 411201, China

Prof. T. Ngai
Department of Chemistry
The Chinese University of Hong Kong
Shatin, N.T., Hong Kong 999077, China

The ORCID identification number(s) for the author(s) of this article can be found under https://doi.org/10.1002/marc.202000123.

DOI: 10.1002/marc.202000123

ensured by heavy aggregation of hydrophobic AIEgens in the hydrophilic hydrogel matrix rather than the aggregation-caused quenching (ACQ) effect of conventional fluorophores. In this respect, a few impressive recent advances have been achieved by either physical incorporation or chemical graft of such classic AIEgens as tetraphenylethylene (TPE) derivatives and so on.[28–38]

Different from well-known AIE-active TPE fluorophores, the fluorescence nature of naphthalimide (NI) luminogens depends on their chemical structures.[39] For example, the planar N-imide-functionalized NI molecules are reported to be highly fluorescent in solution state, but significantly quench in aggregation state because of dense face-to-face packing (H-aggregation), suggesting the ACQ nature of planar NI molecules. Interestingly, substitution of NI molecules especially with rigid and bulky groups is favorable to disturbing their planarity to produce propeller-shaped molecular conformations,[39–41] which can significantly restrict H-aggregation and thus transform planar ACQ fluorophores into AIE/AIEEgens. This strategy, which potentially resolves the ACQ hurdle of NI molecules by well-designed structural substitution, has been employed by many research groups and significantly extended their potential applications. Up to now, numerous AIE-active fluorescent molecules, polymers and nanoparticles have been fabricated from substituted NI derivatives.[42–47] Their applications range from environmental pollutant detection, biologically active molecule recognition, therapeutics, diagnostics, light-emitting diodes, and so on. However, few attempts have been conducted to introduce this unique NI luminogen into cross-linked polymeric network to prepare highly fluorescent polymeric hydrogels. Such AIE-active polymeric hydrogels with well-tunable emission will be favorable to enlarging the list of fluorescent polymeric hydrogels and producing functional material platform with patterned structure as well as the development of bioinspired synergistic fluorescent actuators.

Herein, we report the facile preparation of naphthalimide-based aggregation-induced emissive polymeric hydrogels, followed by thermoresponsive emission/transmittance functional synergy for fluorescence pattern switching and biomimetic actuating applications. The key step to preparing the hydrogels is synthesis of our new-type AIE-active monomer 4-phenoxy-*N*-allyl-1,8-naphthalimide (PhAN). As shown in **Scheme 1**, rigid phenoxy groups are specially designed to modify NI core to break its planarity to produce desirable propeller-shaped molecular conformation, which renders PhAN AIE nature. Furthermore, the AIE effect of phenoxy-substituted NI fluorophores can be boosted by appending them into a linear polymeric chain (poly(PhAN-NIPAM-HEMA)) through radical copolymerization with *N*-isopropyl acrylamide (NIPAM) and hydroxyethyl methacrylate (HEMA). Therefore, the obtained polymeric PhAN/PNIPAM hydrogels are proved to be typically AIE-type and blue-light-emitting hydrogels, which were prepared by one-pot radical copolymerization of NIPAM, methylene-bis-acrylamide (Bis) in the presence of linear poly(PhAN-NIPAM-HEMA). Interestingly, blue fluorescence of PhAN/PNIPAM hydrogels can be significantly increased by heating-induced volume phase transition (VPT) and heavier aggregation of NI fluorophores, accompanying with large transmittance decrease. This unique hydrogel system

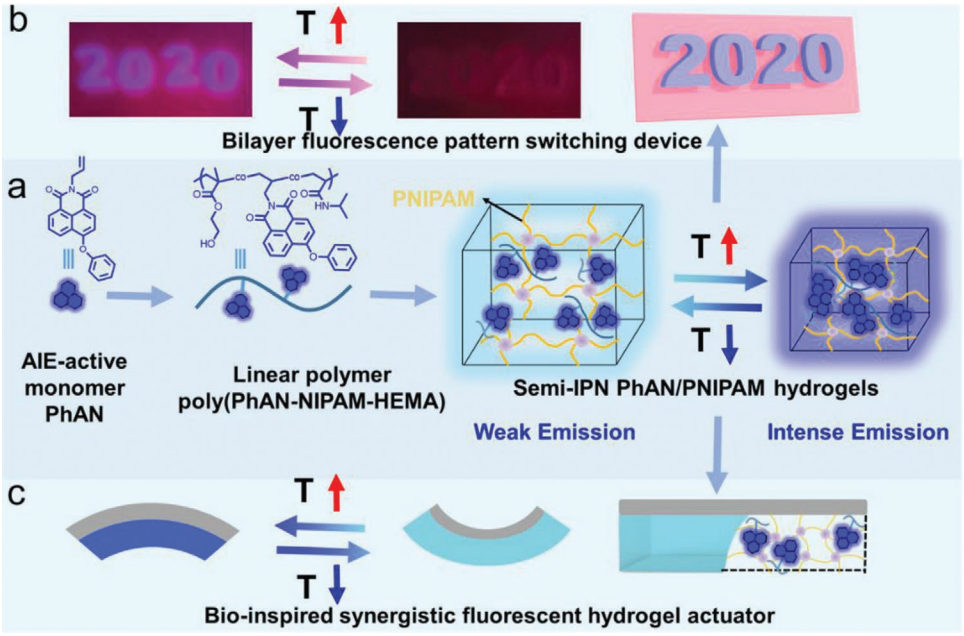

Scheme 1. Illustration of the design and preparation of the AIE-active semi-IPN fluorescent hydrogels and their thermocontrolled emission behavior. Briefly speaking, rigid phenoxy groups are first designed to modify NI core to produce a new AIE-active fluorescent monomer PhAN a). Subsequent radical polymerization of PhAN with NIPAM and HEMA gives a linear fluorescent polymer poly(PhAN-NIPAM-HEMA), which is then interpenetrated into the chemically cross-linked poly(NIPAM) chains via hydrogen bonds to produce Semi-IPN PhAN/PNIPAM hydrogels. Owing to heating-triggered much heavier aggregation of NI fluorophores above volume phase transition temperature (VPTT), this unique hydrogel system is endowed with thermally responsive emission change. As a proof of concept, their potential uses as proto-type fluorescence pattern switching devices b) and biomimetic actuators c) were further demonstrated.

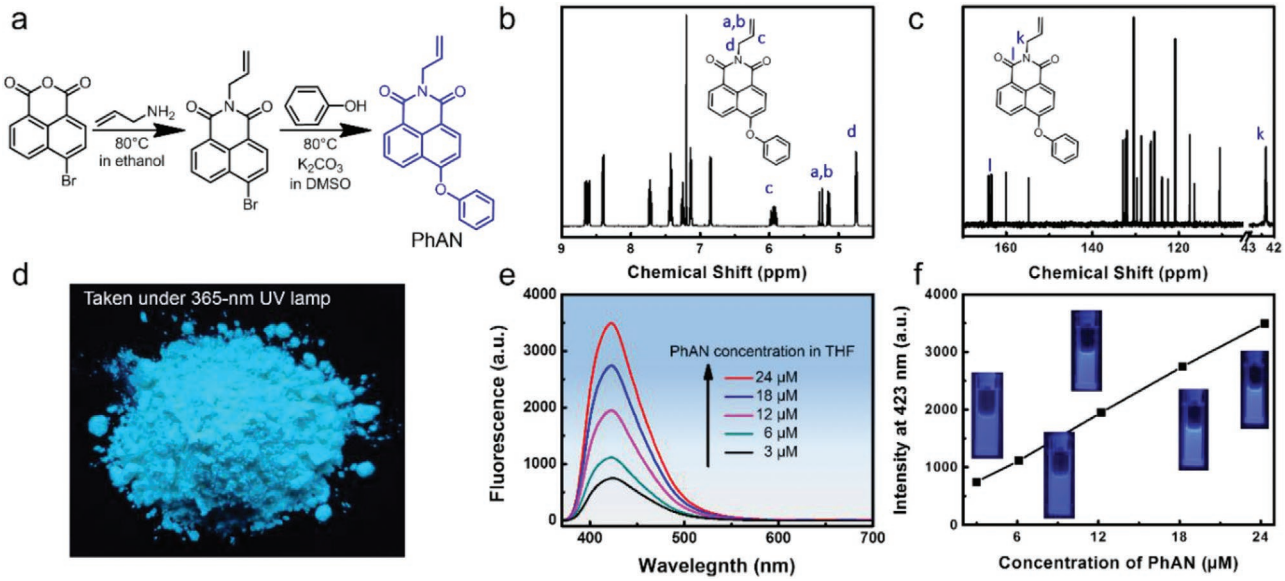

Figure 1. a) Synthetic procedure of the AIE-active monomer PhAN; b) ^{1}H NMR and c) ^{13}C NMR spectra of PhAN recorded in $CDCl_3$; d) the photo of PhAN powder taken under a 365 nm UV lamp; e) fluorescence spectra of PhAN in THF with increasing concentration (excitation at 365 nm); f) peak fluorescence intensity of PhAN as a function of its concentration in THF (inset photos of PhAN solutions at different concentrations taken under a 365 nm UV lamp).

combines the features of thermally responsive fluorescence and transmittance response, thus enabling the simultaneous regulation of two optical properties merely by a single stimulus. As a proof of concept, Atolla Jellyfish-inspired colorful patterned devices with stimuli-responsive fluorescence pattern switching behaviors (Scheme 1b) were fabricated by assembling the developed blue-light-emitting PhAN/PNIPAM hydrogel films onto other red/green-light-emitting hydrogel films. Anisotropic bilayer fluorescent hydrogel actuators (Scheme 1c) were also developed by employing our thermoresponsive PhAN/PNIPAM hydrogel as actuating layer.

The synthetic routes to the AIE-active PhAN monomer is shown in **Figure 1**a. 4-Bromo-1,8-naphthalic anhydride was first obtained according to the reported method[48] and subsequently treated with phenol through the base assisted nucleophilic substitution reaction to give PhAN as a light yellow solid. This specially designed new monomer was characterized by ^{1}H NMR (Figure 1b) and ^{13}C NMR (Figure 1c) spectra. PhAN is readily soluble in common organic solvents (e.g., DMSO, DMF, $CHCl_3$, and THF), but not in deionized water. Its solid powder emits intense blue light under either 365 nm or 254 nm UV light illumination (Figure 1d; Figure S1, Supporting Information). Fluorescence intensities of its THF solutions rise with increasing concentration ranging from 3×10^{-6} to 24×10^{-6} M (Figure 1e,f; Figure S2a,b, Supporting Information). Moreover, an obvious fluorescent emission enhancement could be observed when increasing concentration of PhAN in methanol or the deionized water fraction of methanol/water mixtures, respectively (Figures S3 and S4, Supporting Information). These results clearly demonstrate the AIE nature of the PhAN monomer.

Since PhAN is nearly insoluble in water, it is better to incorporate the AIE-active blue-light-emitting naphthalimide fluorophores into hydrophilic polymers to facilitate synthesis of fluorescent polymeric hydrogels. To this end, PhAN was radically copolymerized with hydrophilic NIPAM and HEMA monomers (molar feed ratio of NIPAM to HEMA is 23:1) by using azobisisobutyronitrile (AIBN) as initiator to produce relatively pure water-soluble poly(PhAN-NIPAM-HEMA) without residual monomer (**Figure 2**a). Considering the relative lower polymerization activity of allyl-type PhAN monomer than acrylamide-like NIPAM monomers, it is quite necessary to completely remove the unreacted PhAN monomer in order to obtain high-purity fluorescent poly(PhAN-NIPAM-HEMA) polymer. Herein, the residual PhAN monomer is removed by precipitation in *n*-hexane because *n*-hexane is a good solvent for PhAN but poor solvent for poly(PhAN-NIPAM-HEMA) polymer (Figures S5 and S6, Supporting Information). The number-average molecular weight of the copolymer is determined to be about 30 000 with a polydispersity index of 1.63 by GPC measurement (Figure S7, Supporting Information). Through the analysis of the UV–vis spectra of monomer and copolymer (Figures S8a,b and S9, Supporting Information), the PhAN content in the prepared copolymer is calculated to be 2.3 wt% according to the reported method.[49] The PhAN content is so slight that it nearly has no influence on the lower critical solution temperature (LCST) behavior of the copolymer, as is evidenced by the result that there is a very sharp volume phase transition (Figure 2b) with an LCST of around 33 °C for aqueous poly(PhAN-NIPAM-HEMA) solution (2 mg mL^{-1}). Notably, aqueous solution of low-concentration poly(PhAN-NIPAM-HEMA) (0.01–0.05 mg mL^{-1}) is nearly nonemissive, while the fluorescence gradually becomes visible at higher concentration (Figure 2c; Figures S10 and S11, Supporting Information), indicating that the phenoxy-substituted naphthalimide luminogen maintains its AIE activity after being incorporated into the polymer chain. Moreover, remarkably enhanced fluorescence emission (more than five

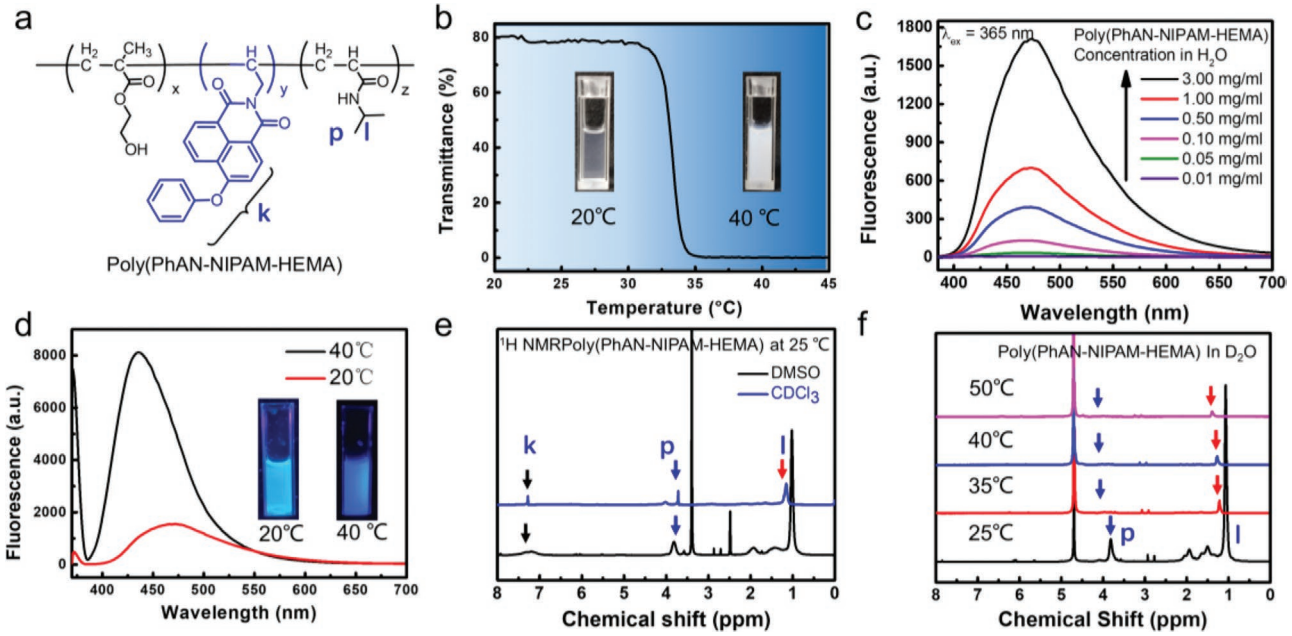

Figure 2. a) Chemical structure of the linear AIE-active polymer poly(PhAN-NIPAM-HEMA); b) temperature-dependent transmittance curve of aqueous poly(PhAN-NIPAM-HEMA) solution (2 mg mL^{-1}), as well as the corresponding photos taken at 20 and 40 °C; c) room-temperature fluorescence spectra of poly(PhAN-NIPAM-HEMA) in water with increasing concentration (excitation at 365 nm); d) fluorescence spectra of aqueous poly(PhAN-NIPAM-HEMA) solution (2 mg mL^{-1}) recorded at 20 and 40 °C (excitation at 365 nm), as well as the corresponding photos taken under a 365 nm UV lamp; e) ^{1}H NMR of poly(PhAN-NIPAM-HEMA) recorded in DMSO-d_6 and $CDCl_3$ at 25 °C; f) temperature-dependent ^{1}H NMR spectra of poly(PhAN-NIPAM-HEMA) measured in D_2O.

times; Figure 2d) is further observed when heating aqueous poly(PhAN-NIPAM-HEMA) solution to above LCST (e.g., 40 °C). To gain more information about the thermal transition of poly(PhAN-NIPAM-HEMA), its ^{1}H NMR spectra were also recorded in DMSO-d_6, $CDCl_3$, and D_2O. Since both DMSO and $CDCl_3$ are good solvents for the polymer chain and phenoxy-substituted NI luminogen, the resonance signals of all protons are visible in the ^{1}H NMR spectrum recorded in DMSO-d_6 and $CDCl_3$ at 25 °C (Figure 2e). However, signals for the aromatic protons ranging from 7 to 8 ppm disappear in D_2O at 25 °C (Figure 2f), which is a poor solvent for NI fluorophore. This is possibly because the hydrophobic NI groups have been wrapped into the hydrophilic polymer coil. At room temperature, the aggregation of NI luminogens must be loose, as is evidenced by the observation that aqueous solution of poly(PhAN-NIPAM-HEMA) is quite transparent (Figure 2b, inset). The loose aggregation results in partially restricted intramolecular rotation of the propeller-shaped NI group, which explains why aqueous solution of poly(PhAN-NIPAM-HEMA) is emissive at room temperature. At elevated temperature, the polymer chain begins to dehydrate and shrink to form compact polymer chain aggregation,[50] as is demonstrated by the downfield shift and intensity decrease in ^{1}H NMR signals of the isopropyl pendants from 25 to 50 °C (Figure 2f). As a result, aqueous solution of poly(PhAN-NIPAM-HEMA) undergoes a thermotriggered volume phase transition and thus becomes opaque. Heavier aggregation of polymer chain significantly activates the restriction of intramolecular rotation process for the grafted NI luminogen, further causing largely enhanced emission.

As shown in **Figure 3**a, the fluorescent PhAN/PNIPAM hydrogels were prepared by one-pot radical copolymerization of NIPAM and methylene-bis-acrylamide (Bis as cross-linker) in the presence of water-soluble poly(PhAN-NIPAM-HEMA) polymer. During the gelation process, linear fluorescent poly(PhAN-NIPAM-HEMA) polymer chains are interpenetrated into the hydrogel matrix by hydrogen bonding with the newly formed poly(NIPAM) chains.[51] For the purpose of modulating fluorescent features via changes in the concentration of linear poly(PhAN-NIPAM-HEMA) polymer, five PhAN/PNIPAM hydrogel samples were synthesized by varying the feed ratio (Table S1, Supporting Information). All of these hydrogel samples are transparent and colorless. Under 365 nm UV light illumination, they can emit weak blue light. Figure 3b and Figure S12 (Supporting Information) present their peak emission intensities and fluorescent spectra at 20 °C. It is found that their room-temperature fluorescence intensities show a significantly positive correlation with the concentrations of linear poly(PhAN-NIPAM-HEMA) polymer, suggesting that the obtained PhAN/PNIPAM hydrogels should be also AIE-active. As expected, remarkably enhanced blue emission is observed when heated (Figure 3b; Figure S13, Supporting Information) because of volume phase transition-triggered naphthalimide fluorophore aggregation. Similar blue-light emission enhancement phenomena were found when excited at 254 nm (Figure S14, Supporting Information).

To clearly explain the thermoresponsive fluorescence response of PhAN/PNIPAM hydrogels, PhAN/PNIPAM-2, which contains 3 mg mL^{-1} linear poly(PhAN-NIPAM-HEMA) polymer, is proved to have the largest emission enhancement

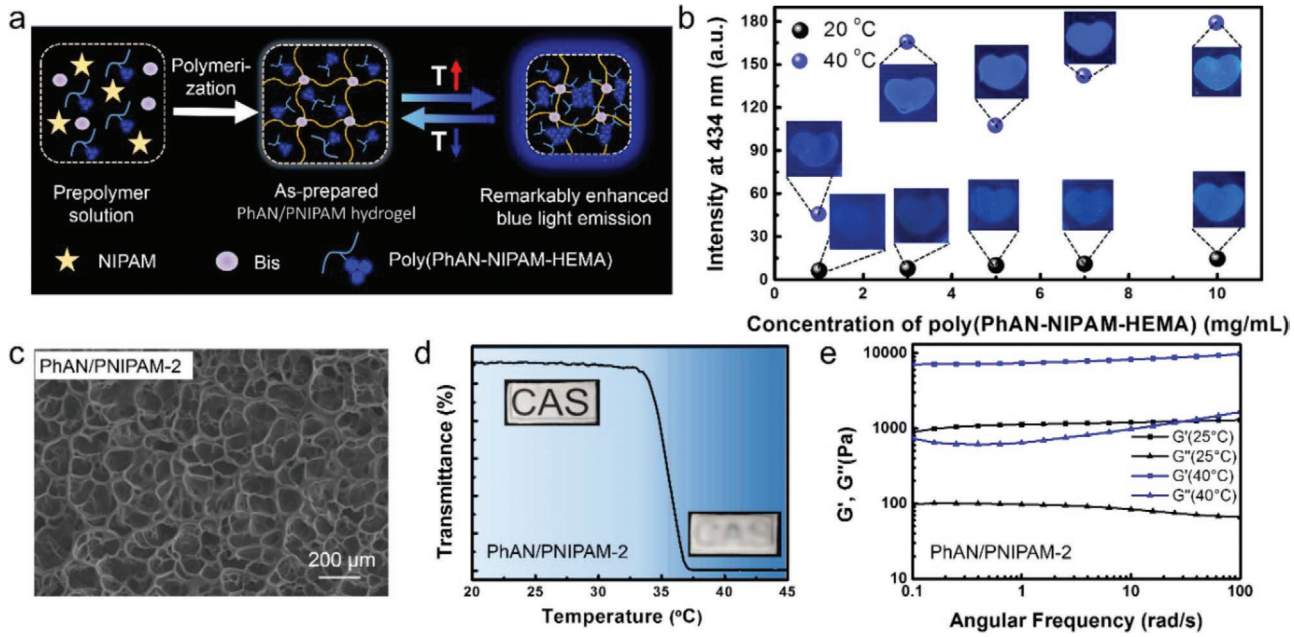

Figure 3. a) Schematic illustration of the synthetic procedure and thermoresponsive fluorescent mechanism of the AIE-active PhAN/PNIPAM hydrogels; b) peak fluorescence intensities of PhAN/PNIPAM hydrogels containing various content of poly(PhAN-NIPAM-HEMA) measured at 20 and 40 °C (excitation at 365 nm), as well as the inset photos of these hydrogel samples taken under a 365 nm UV lamp; c) SEM image of the freeze-dried PhAN/PNIPAM-2 hydrogel; d) temperature-dependent transmittance curve of PhAN/PNIPAM-2 hydrogel, as well as the corresponding photos taken below and above VPTT; e) the rheology measurement of PhAN/PNIPAM-2 hydrogel at 25 and 40 °C.

ratio (Figure 3b) and was thus chosen as an example for systematical investigation. As shown in Figure 3c and Figure S15 (Supporting Information), PhAN/PNIPAM-2 hydrogel has typically porous cross-linked network and can be gradually swollen at cool water (25 °C; Figure S16, Supporting Information). The hydrogel film looks colorless and transparent (Figure 3d, inset). Superior to the traditional single-network PNIPAM hydrogel that is quite brittle,[52] PhAN/PNIPAM-2 hydrogel can be stretched to more than two times its original length (Figure S17, Supporting Information) owing to its semi-IPN structure. Temperature-dependent transmittance measurement (Figure 3d) reveals a distinct transition between 34 and 37 °C with a slightly higher VPTT than LCST of the linear poly(PhAN-NIPAM-HEMA) polymer (about 32 °C). Above VPTT (such as 40 °C), the transparent PhAN/PNIPAM-2 hydrogel film quickly turns to be opaque (Figure 3d, inset), accompanying with a large fluorescence intensity enhancement ratio of more than 19 (Figure S18, Supporting Information). These observations are consistent with the results of rheological tests, in which much higher modulus and toughness at 40 °C clearly demonstrate more compact polymer aggregation caused by volume phase transition (Figure 3e).

The developed hydrogel systems with synergistic and reversible fluorescence/transmittance change can serve well for the development of new-type smart material platforms for potential fluorescence pattern switching applications, including smart displays, anticounterfeit and message storage.[53] As shown in **Figure 4**, the developed PhAN/PNIPAM-2 hydrogel can be facilely tailored into different shapes and patterns because of its freestanding and not bad mechanical properties. These tailored hydrogels were then assembled onto another nonresponsive red-light-emitting fluorescent hydrogel film (see Figure S19 in the Supporting Information for detailed chemical information) to produce bilayer patterned devices. As can be seen in Figure 4a–c, the whole bilayer system emits red fluorescence under UV illumination (254 nm) at room temperature. No patterned information is observed, because our PhAN/PNIPAM-2 hydrogel is transparent and nearly nonfluorescent at room temperature. After being heated, the PhAN/PNIPAM-2 hydrogel pattern begins to emit gradually enhanced blue-light fluorescence, accompanying with large transmittance decrease that can partially block the background red-light emission. As a result, the predesigned fluorescent pattern gradually appears to be violet (from the combination of blue and red) and can be clearly identified by naked eyes because the rest still emits red fluorescence. Similar fluorescence pattern switching behaviors could be realized by assembling patterned PhAN/PNIPAM-2 hydrogel onto green-light-emitting or multicolor fluorescent hydrogel films (Figure 4d; Figures S20 and S21, Supporting Information). Moreover, owing to the highly reversible fluorescence and transmittance change of PhAN/PNIPAM-2 hydrogel, these fluorescent patterns could be dynamically displayed by heating above VPTT and then erased by cooling to room temperature. Such spatial/temporal emission control is beneficial to produce fluorescent hydrogels with patterned heterogeneities and periodicities, providing specific areas with disparate functions. Therefore, these fluorescent pattern switching devices are expected to hold great potential for many applications, including sensing chips, data encryption, storage, and displays.[54,55]

Fluorescent polymeric hydrogels with bioinspired synergistic shape changing functions are also of significant

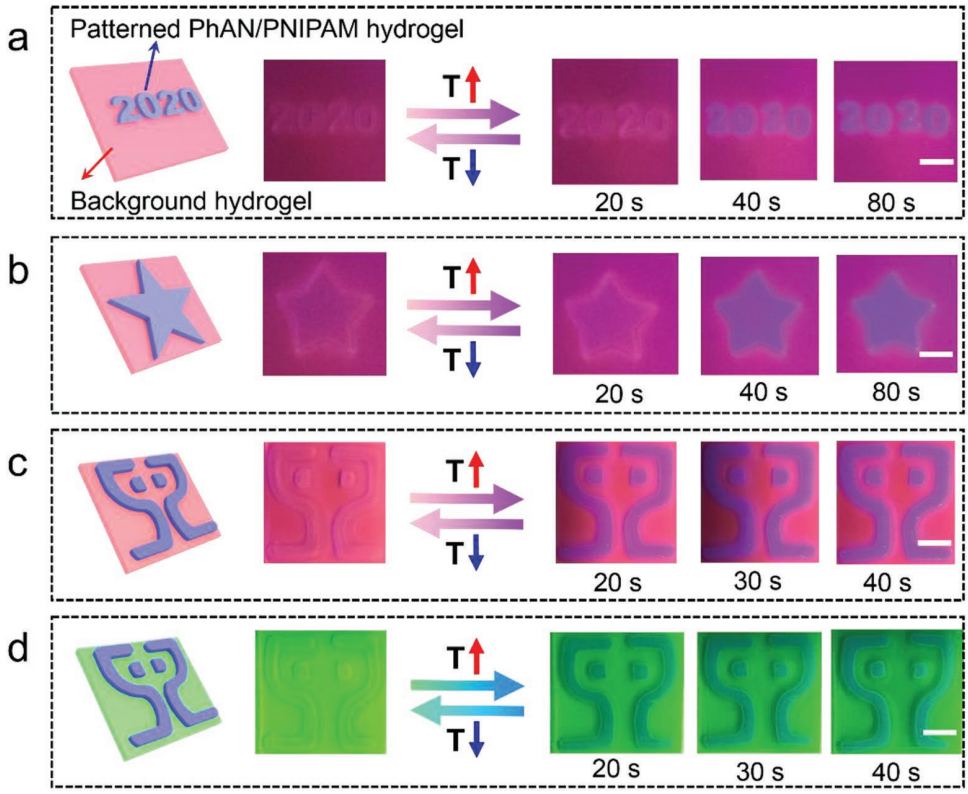

Figure 4. Thermocontrolled bilayer fluorescence pattern switching devices, which are prepared by assembling patterned PhAN/PNIPAM-2 hydrogels onto nonresponsive red-light-emitting hydrogel (a–c) or green-light-emitting hydrogel (d). These photos are taken under a 254 nm UV lamp (scale bar, 1 cm).

research interest because such multifunctional synergy of optical and transformable features is favorable to yielding powerful life-like soft actuators/robotics (e.g., camouflaged robots).[52,56] Therefore, enlightened by both thermotriggered volume phase transition and fluorescence enhancement of our PhAN/PNIPAM hydrogels, we sought to further exploit their potential application as fluorescent hydrogel actuators. As presented in **Figure 5**a, the anisotropic bilayer actuator was produced by utilizing PhAN/PNIPAM-2 hydrogel film as the actuating layer and pan paper as a passive layer by using our reported method.[52] Its anisotropic actuation behavior is caused by the mismatch of thermoregulated swelling ratio and modules of bilayers. When placed in cool water (20 °C), the straight weakly fluorescent bilayer actuator rapidly absorb water to swell and curl to be circle-shaped. To quantitatively study its thermocontrolled actuating process, this circle-shaped actuator with the hydrogel layer on the out face was put into hot water (40 °C) and the bending angle (θ) change was recorded real-timely. As summarized in Figure 5b, its bending angle gradually decreases from above 300° to nearly 0° within 300 s and then decreases to about −300° at 540 s owing to the thermoregulated deswelling behavior of our PhAN/PNIPAM-2 hydrogel layer. Notably, this reversible shape-morphing behavior is accompanied with simultaneous optical change (fluorescence enhancement and transmittance decrease), just like the well-known camouflaging ability of marine Watasenia Scintillans that are realized by synergistic shape and skin color manipulation. This bioinspired actuator design is of interest, as it may pave the way for accessible color-changing soft robots that are expected to be widely useful in various scientific fields.

In summary, we have presented synthesis and potential application of new-type naphthalimide-based aggregation-induced emissive polymeric hydrogels with thermally tunable fluorescence and transmittance. Their typical AIE-active fluorescence derives from our specially designed PhAN monomer, in which bulky and rigid phenoxy substitution groups are employed to disturb the planarity of NI fluorophores to produce propeller-shaped molecular conformation that is favorable for aggregation-induced emission. The blue fluorescence of our as-prepared PhAN/PNIPAM hydrogels can be further significantly enhanced at a temperature above VPTT owing to much denser aggregation of hydrophobic phenoxy-substituted NI fluorophores. In other words, the developed PhAN/PNIPAM hydrogels are characterized with simultaneous modulation of both fluorescence and transmittance properties by the same stimulus. This work will enlarge the list of stimuli-responsive fluorescent polymeric hydrogels. Moreover, their useful features may also extend their potential use as novel smart optical platform for various applications (e.g., anticounterfeit, sensors, display, and actuators), as is evidenced by the fabrication of several proto-type fluorescence pattern switching and biomimetic actuating devices.

Experimental Section

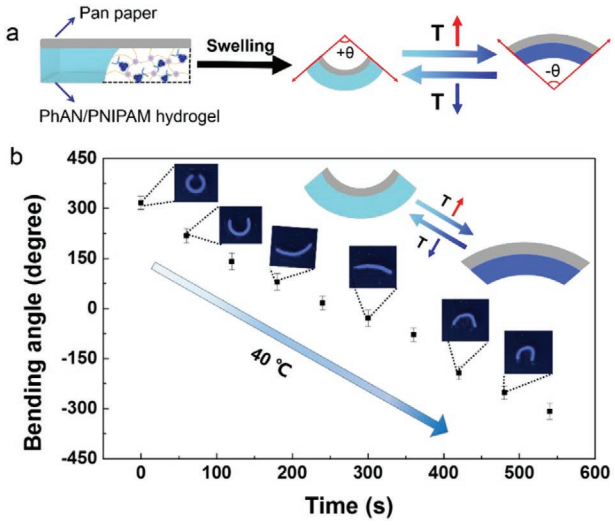

Figure 5. Anisotropic bilayer actuator with thermoregulated synergistic shape-morphing and fluorescence switching behavior. a) Schematic illustration of the bilayer actuator and its thermocontrolled actuating process; b) time-dependent bending angles of the designed bilayer actuator in hot water, as well as the corresponding photos taken at different time intervals. (Although the bending angle change is obvious, the optical changes seems not obvious. In fact, both the thermotriggered fluorescence enhancement and transmittance loss of the as-prepared bilayer actuators are obvious, as is demonstrated by the results summarized in Figure 3b,d. However, since the hydrogel layer of the actuator is quite thin (0.5 mm) and narrow (2 mm), the optical changes may not be clearly recorded by our smart phone camera (Xiaomi 8). Additionally, visual noise may also be caused by the passive layer (pan paper) that can slightly reflect the excitation or emission light. These reasons together possibly result in the observation that the optical change seems not obvious in (b).

Materials: Ammonium persulfate (APS), allylamine, and *N*,*N*′-methylene bis(acrylamide) (Bis) were purchased from Aladdin Chemistry Co., Ltd. 4-Bromo-1,8-naphthalic anhydride were purchased from Energy Chemical Co. *N*-Isopropyl acrylamide and hydroxyethyl methacrylate were commercially provided by Tokyo Chemical Industry Co. Ltd. Phenol, potassium carbonate, dioxane, and ethanol were obtained from Sinopharm Chemical Reagent Co. Ltd. Anhydrous dimethyl sulfoxide (DMSO) was provided by J&K Scientific Ltd.

Synthesis of the AIE-Active Monomer 4-Phenoxy-N-allyl-1,8-naphthalimide (PhAN): 4-Bromo-*N*-allyl-1,8-naphthalimide was first synthesized by using the reported method.[48] And, then 0.316 g 4-bromo-*N*-allyl-1,8-naphthalimide (1 mmol), 0.188 g phenol (2 mmol), 0.414 g potassium carbonate (3 mmol), and 20 mL anhydrous DMSO were added to a 50 mL three-necked flask under N_2 protection. After being stirred at 80 °C for 12 h, a large amount of deionized water (150 mL) was added to terminate the reaction. The mixture was then extracted by CH_2Cl_2 for three times and washed with aqueous NaOH solution (1 mg mL^{-1}) to remove the residual phenol. Anhydrous sodium sulfate was added to the organic phase to remove the residual water. PhAN was finally obtained as a yellow power in 50.5% yield after removing the solvent under vacuum. ^{1}H NMR (400 MHz, CDCl3): 4.82 (d, CH–CH_2–N), 5.20–5.25 (d, CH_2–CH–), 5.30–5.37 (d, CH_2–CH–), 6.02 (m, CH_2–CH–), 6.93 (d, Ar–H), 7.19–7.24 (d, Ar–H), 7.30–7.36 (m, Ar–H), 7.46–7.54 (m, Ar–H), 7.78–7.82 (m, Ar–H), 8.46–8.50 (d, Ar–H), 8.71 (d, Ar–H), 8.78 (d, Ar–H).

Preparation of the Linear Poly(PhAN-NIPAM-HEMA) Polymer: Under N_2 atmosphere, PhAN (30 mg, 0.09 mmol), HEMA (50 mg, 0.38 mmol), NIPAM (1 g, 8.8 mmol), and AIBN (11 mg) were dissolved in 6 mL dioxane. After being polymerized at 80 °C for 8 h, the mixture was added to hexane (30 mL) dropwise to precipitate the linear polymer. Poly(PhAN-NIPAM-HEMA) was finally collected as a white solid in 80.5% yield after being filtered and dried under vacuum at room temperature for 12 h.

Preparation of the Fluorescent PhAN/PNIPAM Hydrogels: In a typical experiment, NIPAM (975 mg), Bis (5 mg), APS (10 mg), linear poly(PhAN-NIPAM-HEMA) polymer (2.15 mL, 10 mg mL^{-1}), and 5 mL deionized water were mixed. After being shaken to completely dissolve in a refrigerator (–4 °C), the accelerator *N*,*N*,*N*′,*N*′-tetramethylethylenediamine (TEMED, 7.15 µL) was added and well mixed. Finally, the precursor solution was placed into the self-prepared molds with two glass plates and one 0.5 mm thick silicon plate and polymerized at 10 °C for 12 h to produce the fluorescent PhAN/PNIPAM hydrogels. Different PhAN/PNIPAM hydrogel samples (see Table S1 in the Supporting Information for detailed information) were prepared by varying the feed volume of the linear poly(PhAN-NIPAM-HEMA) polymer.

Characterization: ^{1}H NMR and ^{13}C NMR spectra of PhAN and poly(PhAN-NIPAM-HEMA) polymer were recorded on Bruker Advance AMX-400 Spectrometer in $CDCl_3$, DMSO-d_6 or D_2O by using tetramethylsilane as the internal reference. Fluorescence spectra of the poly(PhAN-NIPAM-HEMA) polymer and PhAN/PNIPAM hydrogels were measured by Hitachi F-4600 Spectrofluorometer equipped with a xenon (Xe) lamp (150 W). UV–vis spectra were obtained on a PerkinElmer Lambda 950 UV–vis–NIR spectrometer in a 10 mm path length cell. ATR-FT-IR spectra of the freeze-dried hydrogel samples were recorded on a Micro FT-IR (Cary 660+620) instrument. Surface and cross section morphology of the freeze-dried PhAN/PNIPAM hydrogels were performed by a field-emission scanning electron microscopy (SEM, S-4800, Hitachi) with an accelerating voltage of 5.0 kV. Digital photos were taken by our smart phone (Xiaomi 8).

Supporting Information

Supporting Information is available from the Wiley Online Library or from the author.

Acknowledgements

H.L. and S.W. contributed equally to this work. The authors are grateful for the financial support from the National Natural Science Foundation of China (21774138, 51773215, 51873223), Key Research Program of Frontier Sciences, Chinese Academy of Sciences (QYZDB-SSW-SLH036), Youth Innovation Promotion Association of Chinese Academy of Sciences (2019297, 2017337), Ningbo Scientific and Technological Innovation 2025 Major Project (2018B10057), and the Open Research Fund of Key Laboratory of Marine Materials and Related Technologies (2018K02).

Conflict of Interest

The authors declare no conflict of interest.

Keywords

actuators, aggregation-induced emission, fluorescent hydrogels, naphthalimide

Received: March 9, 2020
Revised: April 26, 2020
Published online: May 13, 2020

[1] E. A. Widder, *Science* **2010**, *328*, 704.

[2] X. Le, W. Lu, J. Zhang, T. Chen, *Adv. Sci.* **2019**, *6*, 1801584.
[3] H. Wei, S. Du, Y. Liu, H. Zhao, C. Chen, Z. Li, J. Lin, Y. Zhang, J. Zhang, X. Wan, *Chem. Commun.* **2014**, *50*, 1447.
[4] S. Bhattacharya, R. S. Phatake, S. Nabha Barnea, N. Zerby, J. J. Zhu, R. Shikler, N. G. Lemcoff, R. Jelinek, *ACS Nano* **2019**, *13*, 7396.
[5] N. Goswami, F. Lin, Y. Liu, D. T. Leong, J. Xie, *Chem. Mater.* **2016**, *28*, 4009.
[6] M. Liras, I. Quijada-Garrido, O. García, *Polym. Chem.* **2017**, *8*, 5317.
[7] M. Wang, X. Li, W. Hua, L. Shen, X. Yu, X. Wang, *ACS Appl. Mater. Interfaces* **2016**, *8*, 23995.
[8] Z. Li, Z. Hou, H. Fan, H. Li, *Adv. Funct. Mater.* **2017**, *27*, 1604379.
[9] Q. Zhu, K. Vliet, N. Holten-Andersen, A. Miserez, *Adv. Funct. Mater.* **2019**, *29*, 1808191.
[10] H. Zhi, X. Fei, J. Tian, M. Jing, L. Xu, X. Wang, D. Liu, Y. Wang, J. Liu, *J. Mater. Chem. B* **2017**, *5*, 5738.
[11] Q.-F. Li, X. Du, L. Jin, M. Hou, Z. Wang, J. Hao, *J. Mater. Chem. C* **2016**, *4*, 3195.
[12] M. X. Wang, C. H. Yang, Z. Q. Liu, J. Zhou, F. Xu, Z. Suo, J. H. Yang, Y. M. Chen, *Macromol. Rapid Commun.* **2015**, *36*, 465.
[13] D. Fan, X. Fei, J. Tian, H. Zhi, L. Xu, X. Wang, Y. Wang, *Polym. Chem.* **2016**, *7*, 3766.
[14] C. N. Zhu, T. Bai, H. Wang, W. Bai, J. Ling, J. Z. Sun, F. Huang, Z. L. Wu, Q. Zheng, *ACS Appl. Mater. Interfaces* **2018**, *10*, 39343.
[15] Y. Zhang, X. Le, Y. Jian, W. Lu, J. Zhang, T. Chen, *Adv. Funct. Mater.* **2019**, *29*, 1905514.
[16] Y. Zhang, Y. Chen, J. Li, L. Liang, Y. Liu, *Acta Chim. Sin.* **2018**, *76*, 622.
[17] H. Chen, F. Yang, Q. Chen, J. Zheng, *Adv. Mater.* **2017**, *29*, 1606900.
[18] X. Ji, R. T. Wu, L. Long, X. S. Ke, C. Guo, Y. J. Ghang, V. M. Lynch, F. Huang, J. L. Sessler, *Adv. Mater.* **2018**, *30*, 1705480.
[19] K. Benson, A. Ghimire, A. Pattammattel, C. V. Kumar, *Adv. Funct. Mater.* **2017**, *27*, 1702955.
[20] H. Chen, X. Ma, S. Wu, H. Tian, *Angew. Chem., Int. Ed.* **2014**, *53*, 14149.
[21] H. S. Peng, J. A. Stolwijk, L. N. Sun, J. Wegener, O. S. Wolfbeis, *Angew. Chem., Int. Ed.* **2010**, *49*, 4246.
[22] C. Zhang, Y. Li, X. Xue, P. Chu, C. Liu, K. Yang, Y. Jiang, W. Q. Chen, G. Zou, X. J. Liang, *Chem. Commun.* **2015**, *51*, 4168.
[23] H. Jia, Z. Li, X. Wang, Z. Zheng, *J. Mater. Chem. A* **2015**, *3*, 1158.
[24] C. Belger, J. G. Weis, E. Egap, T. M. Swager, *Macromolecules* **2015**, *48*, 7990.
[25] D. Wang, T. Liu, J. Yin, S. Liu, *Macromolecules* **2011**, *44*, 2282.
[26] X. Zhang, K. Wang, M. Liu, X. Zhang, L. Tao, Y. Chen, Y. Wei, *Nanoscale* **2015**, *7*, 11486.
[27] Y. Xia, B. Xue, M. Qin, Y. Cao, Y. Li, W. Wang, *Sci. Rep.* **2017**, *7*, 9691.
[28] J. M. Galindo, J. Leganés, J. Patiño, A. M. Rodríguez, M. A. Herrero, E. Díez-Barra, S. Merino, A. M. Sánchez-Migallón, E. Vázquez, *ACS Macro Lett.* **2019**, *8*, 1391.
[29] X. Ji, Z. Li, X. Liu, H. Q. Peng, F. Song, J. Qi, J. W. Y. Lam, L. Long, J. L. Sessler, B. Z. Tang, *Adv. Mater.* **2019**, *31*, 1902365.
[30] Z. Wang, J. Nie, W. Qin, Q. Hu, B. Z. Tang, *Nat. Commun.* **2016**, *7*, 12033.
[31] L. Shao, J. Sun, B. Hua, F. Huang, *Chem. Commun.* **2018**, *54*, 4866.
[32] H. Wang, X. Ji, Y. Li, Z. Li, G. Tang, F. Huang, *J. Mater. Chem. B* **2018**, *6*, 2728.
[33] Y. Lin, C. Li, G. Song, C. He, Y. Q. Dong, H. Wang, *J. Mater. Chem. C* **2015**, *3*, 2677.
[34] X. Wang, K. Xu, H. Yao, L. Chang, Y. Wang, W. Li, Y. Zhao, J. Qin, *Polym. Chem.* **2018**, *9*, 5002.
[35] F. Ishiwari, H. Hasebe, S. Matsumura, F. Hajjaj, N. Horii-Hayashi, M. Nishi, T. Someya, T. Fukushima, *Sci. Rep.* **2016**, *6*, 24275.
[36] S. S. Liow, Q. Dou, D. Kai, Z. Li, S. Sugiarto, C. Y. Yu, R. T. Kwok, X. Chen, Y. L. Wu, S. T. Ong, A. Kizhakeyil, N. K. Verma, B. Z. Tang, X. J. Loh, *Small* **2017**, *13*, 1603404.
[37] Z. Li, P. Liu, X. Ji, J. Gong, Y. Hu, W. Wu, X. Wang, H. Q. Peng, R. T. K. Kwok, J. W. Y. Lam, J. Lu, B. Z. Tang, *Adv. Mater.* **2020**, *32*, 1906493.
[38] B. Li, Y. Zhang, B. Yan, D. Xiao, X. Zhou, J. Dong, Q. Zhou, *RSC Adv.* **2020**, *10*, 7118.
[39] P. Gopikrishna, N. Meher, P. K. Iyer, *ACS Appl. Mater. Interfaces* **2018**, *10*, 12081.
[40] J. Mei, Y. Hong, J. W. Lam, A. Qin, Y. Tang, B. Z. Tang, *Adv. Mater.* **2014**, *26*, 5429.
[41] J. Mei, N. L. Leung, R. T. Kwok, J. W. Lam, B. Z. Tang, *Chem. Rev.* **2015**, *115*, 11718.
[42] R. Hu, N. L. Leung, B. Z. Tang, *Chem. Soc. Rev.* **2014**, *43*, 4494.
[43] Y. Bao, H. De Keersmaecker, S. Corneillie, F. Yu, H. Mizuno, G. Zhang, J. Hofkens, B. Mendrek, A. Kowalczuk, M. Smet, *Chem. Mater.* **2015**, *27*, 3450.
[44] H. H. Lin, Y. C. Chan, J. W. Chen, C. C. Chang, *J. Mater. Chem.* **2011**, *21*, 3170.
[45] N. Meher, S. R. Chowdhury, P. K. Iyer, *J. Mater. Chem. B* **2016**, *4*, 6023.
[46] P. Y. Gu, C. J. Lu, Z. J. Hu, N. J. Li, T.-T. Zhao, Q. F. Xu, Q. H. Xu, J. D. Zhang, J. M. Lu, *J. Mater. Chem. C* **2013**, *1*, 2599.
[47] X. Cao, N. Zhao, H. Lv, Q. Ding, A. Gao, Q. Jing, T. Yi, *Langmuir* **2017**, *33*, 7788.
[48] P. Li, D. Zhang, Y. Zhang, W. Lu, J. Zhang, W. Wang, Q. He, P. Théato, T. Chen, *ACS Macro Lett.* **2019**, *8*, 937.
[49] W. Lu, P. Xiao, Z. Liu, J. Gu, J. Zhang, Y. Huang, Q. Huang, T. Chen, *ACS Appl. Mater. Interfaces* **2016**, *8*, 20100.
[50] L. Tang, J. K. Jin, A. Qin, W. Zhang Yuan, Y. Mao, J. Mei, J. Zhi Sun, B. Zhong Tang, *Chem. Commun.* **2009**, *45*, 4974.
[51] Y. Liu, K. Zhang, J. Ma, G. J. Vancso, *ACS Appl. Mater. Interfaces* **2017**, *9*, 901.
[52] S. Wei, W. Lu, X. Le, C. Ma, H. Lin, B. Wu, J. Zhang, P. Theato, T. Chen, *Angew. Chem., Int. Ed.* **2019**, *58*, 16243.
[53] M. Xie, F. Xu, L. Zhang, J. Yin, X. Jiang, *ACS Macro Lett.* **2018**, *7*, 540.